Patch Antennas on Externally Perforated High Dielectric Constant Substrates

Joseph S. Colburn, *Member, IEEE*, and Yahya Rahmat-Samii, *Fellow, IEEE*

***Abstract*—Smaller physical size and wider bandwidth are two antenna engineering goals of great interest in the wireless world. To this end, the concept of external substrate perforation is applied to patch antennas in this paper. The goal was to overcome the undesirable features of thick and high dielectric constant substrates for patch antennas without sacrificing any of the desired features, namely, small element size and bandwidth. The idea is to use substrate perforation exterior to the patch to lower the effective dielectric constant of the substrate surrounding the patch. This change in the effective dielectric constant has been observed to help mitigate the unwanted interference pattern of edge diffraction/scattering and leaky waves. The numerical data presented in this paper were generated using the finite-difference time-domain (FDTD) technique. Using this numerical method, a patch antenna was simulated on finite-sized ground planes of two different substrate thicknesses, with and without external substrate perforation. The computations showed the directivity drop in the radiation pattern caused by substrate propagation was noticeably improved by introducing the substrate perforation external to the patch for the case of a patch antenna on a relatively thick substrate without any loss of bandwidth. Measurements of a few patch antennas fabricated on high dielectric constant substrates with and without substrate perforation are included for completness. Good correlation between the computed results and mesurements is observed.**

***Index Terms*—FDTD, high dielectric constant substrates, integrated antennas, patch antennas, substrate perforation, substrate propagation.**

I. Introduction

FABRICATING patch antennas on high dielectric substrates is of growing interest. Patch antennas on high dielectric constant substrates have the benefit of reduced element size due to the shorter wavelengths in such materials and resonant nature of the patch radiator. Besides the main drive of reduced element size, being able to integrate a patch antenna directly on a monolithic microwave integrated circuit (MMIC) substrate simplifies interconnection of the antenna with the circuitry and fabrication. These miniaturized radiators are potentially useful in many applications, from small personal communication and global positioning system (GPS) transceivers/receivers to large satellite communication and radar arrays.

But there are drawbacks with the use of high dielectric constant substrates with patch antennas that has inhibited its use. These drawbacks are a result of the tendency for more of the energy delivered to the antenna to be trapped in substrates of higher dielectric constant. This manifests itself in two ways, more tightly coupled, higher Q patch resonators and more of the total energy being trapped in substrate modes, i.e., surface waves and leaky waves. The higher Q patch resonator results in narrower bandwidths. The increase in energy trapped in the substrate modes lowers efficiencies due to losses in the substrate and causes pattern/polarization degradation from the diffraction/scattering of these substrate modes at the finite substrate's edges. To increase the bandwidth of the patch a thicker substrate can be used, but this will increase the amount of energy trapped in the substrate.

Recently, there has been some work directed at overcoming the drawbacks of patch antennas on high dielectric constant material by manipulating the antenna's substrate. One approach suggested was to construct a complete band gap structure surrounding the patch antenna to prevent energy from being trapped in the substrate [1]–[3]. Unfortunately, to form a band gap in the substrate via periodic holes requires considerable area, which may make it impractical for some applications. Typically, to form a band gap at least three periods are required with a period being on the order of a wavelength.

Another approach considered has been to lower the effective dielectric constant of substrate under the patch to allow for more effective radiation [4]–[8]. A drawback to this approach is that the resulting patch antenna has to be larger than a patch on the unperturbed substrate. Also, manipulation of the substrate underneath the patch element makes fabrication more difficult.

In this work, a hybridization of the two above approaches is suggested to help facilitate patch antennas on high dielectric constant substrates; that is, the substrate under the patch is left unperturbed, thus, not increasing the patch size and the substrate surrounding the patch is manipulated to lower its effective dielectric constant to reduce the undesired effects of surface waves. The idea is the change in effective dielectric constant from high under the patch to lower surrounding the patch would inhibit propagation in the substrate and give a degree of control to vary the diffraction/scattering points. With the edge diffraction effects controlled, the substrate thickness can be increased to improve the bandwidth of the patch.

To lower the effective dielectric constant of the substrate, substrate perforation is explored. Substrate perforation is a technique that can be used to lower the effective dielectric constant by creating an array of relatively small closely spaced

Manuscript received September 25, 1998; revised May 31, 1999. This work is based upon work supported in part by the U.S. Army Research Office under Contract DAAH04-96-1-0389.

The authors are with the Department of Electrical Engineering, University of California, Los Angeles, CA, 90095-1594 USA.

Publisher Item Identifier S 0018-926X(99)09980-9.

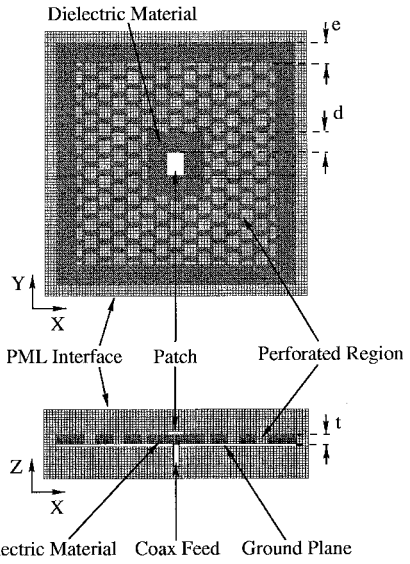

Fig. 1. Schematic of the patch antenna and externally perforated substrate on a finite ground plane. The grid represents the FDTD computational cells.

holes in the substrate [8], [9]. If the hole diameter and spacing remains less than a half-wavelength inside the dielectric material, it has been observed that the effective dielectric constant of the substrate will approximately be the volumetric average of the free-space holes and the remaining dielectric material [10]. This volumetric average model has been found to be insensitive to the exact hole geometry. This approach for lowering the dielectric constant of the surrounding substrate material has the advantage over using different substrate materials to create the same effect because it is monolithic in nature and can be realized using micromaching techniques. Also, using this technique there is considerable freedom in the range of lower effective dielectric constant values achievable by simple choice of the perforation geometry.

The numerical results presented in this work were generated using the finite-difference time-domain (FDTD) technique. The computational code used was a Cartesian grid based implementation with the perfectly matched layer (PML) boundary condition. In all the simulations a uniform $0.02\lambda_o$ ($\lambda_o =$ free-space wavelength) discritization was used. The coax feed model suggested in [11] was used to excite the patch antennas studied.

A few antennas were fabricated on Rogers RT/Duroid 6010 ($\epsilon_r = 10.2$) with and without perforations. The measured resonant frequencies and radiation patterns of these fabricated antennas matched the simulated results well.

II. Patch Antenna with External Perforation

Fig. 1 is a diagram of the geometry of interest, which is a patch antenna on a finite ground plane. The relative dielectric constant of 10.2 was chosen for the substrate. This choice of relative dielectric constant was intended to be representative of silicon or gallium arsenide substrates. Numerical results for two different thicknesses of substrate are shown in this paper, 1 mm and 2 mm. For both of these substrates, the lowest order resonance of the 4 mm $\times$ 3 mm patch antenna simulated is below the cutoff frequency of the TE_1 mode, so only the TM_0 will exist in these substrates at the frequencies of interest [12], which is a common criteria in patch antenna design. The cutoff frequencies of the TE_1 mode for the 1 and 2 mm substrates are 24.7 and 12.4 GHz, respectively. Although both substrates only support the TM_0 mode in the region of the first resonance of the patch, in the thicker substrate, substrate mode effects are expected to be more significant [13].

In the simulations, finite ground plane sizes of approximately $1.2\lambda_o$ and $1.4\lambda_o$ were used. These ground plane sizes were chosen to illustrate how edge diffraction/scattering from substrate modes affect the far-field radiation pattern. For each case simulated, the far-field patterns were computed at the resonant frequency of the patch. This means the physical size of the ground planes was adjusted appropriately to keep its electrical size fixed for all the cases. Note, the electrical size of the ground plane largely determines the interference pattern of the edge diffracted/scattering field and the field radiated directly from the patch.

The intent of this work was to study the effect of substrate perforation on the performance of the patch antennas on finite-sized ground planes. The substrate perforation considered is a two-dimensional array of holes in the substrate surrounding the patch antenna. Each hole simply consists of removal of the dielectric material down to the ground plane. In this work, the hole cross sections are square in shape—2 mm on each side. Within each column, the hole center to center distance is 3 mm and the column to column center separation is 2.5 mm. Adjacent columns of holes are shifted 1.5 mm in y with respect to each other. In all the simulations presented in this paper, the resonance frequency of the patch antenna is within the range of 8.7 to 9.6 GHz, thus, in all cases, the hole size and separation are less than $\lambda_{10.2}/2$ ($\lambda_{10.2} =$ wavelength in material with a dielectric constant of 10.2).

Because of fringing fields, the holes in the substrate are introduced at a distance d from edge of the patch, as shown in Fig. 1. The smallest distance d, which does not cause any increase in the resonance frequency is of interest because it is not desirable to increase the size of the patch.

Another parameter that was studied is the dimension labeled e in Fig. 1, which is a measure of the distance from the edge of the ground plane to the point at which the perforation is stopped. For the case of $e = 0$ mm, the perforation is extended all the way to the edge of the ground plane.

III. Far-Field Radiation Contribution from Edge Diffraction

Finite-sized ground planes influence the radiation pattern of patch antennas. Diffraction/scattering from the edges of finite ground planes have a significant impact on the far-field radiation from patch antennas. These edge diffracted/scattered fields have contributions from three sources; surface waves, space waves, and leaky waves [14]. The relative contributions from each of these sources vary depending on the geometry considered. The contribution to the far-field radiation from edge diffraction/scattering in general is not desirable because

it is difficult to control, thus cannot be effectively used to design for specific pattern or polarization properties.

In many cases, the contribution from surface waves are the dominate component of the edge diffracted/scattered fields. Surface waves are modes in the substrate that do not radiate as they propagate but, at the ground plane edges, the energy trapped in these modes scatter and contribute to the far-field. Thicker and/or higher dielectric constant substrates trap more of the energy into these mode, thus, for these geometries, their effects are more significant. Lossy substrates will reduce their contribution to the far-field radiation pattern, but this energy trapped in the substrate is wasted.

The space waves that diffract from the edges are fields radiated by the patch directly into free-space that are incident upon the ground plane edge. Although this contribution to the diffracted field can never be eliminated, space waves decay faster with distance from the patch than surface waves and, thus, their contribution is proportionally less for increased ground-plane size.

Leaky waves are substrate modes that radiate as they propagate and, hence, contribute directly to the far-field pattern. In addition, when they are incident upon an edge, they contribute to the diffracted/scattered fields. Because they radiate energy as they propagate, their contribution to the edge scattered field decrease as the ground plane size increases. Additionally, lossy substrates will decrease their edge scattered field contributions, but again at the cost of wasted power.

Without special edge treatment, edge diffraction/scattering effects cannot be eliminated [15], [16]. The suggested edge treatment consists of absorbing the substrate mode energy in a lossy material, which itself is not desirable because this energy is thereby wasted, thus decreasing the antenna efficiency.

In this work, the goal was to reduce the undesirable effects of strong edge diffraction/scattering by a combination of reducing the propagation in the substrate and shifting the diffraction/scattering points, thus giving a new control to vary the resulting interference pattern. The substrate propagation is reduced by lowering the effective dielectric constant of the substrate surrounding the patch antenna, this change in impedance will hinder the substrate propagation although it still exists. In addition to the reduction in magnitude of these contributions, with proper choice of the dielectric constant profile, the resulting interference pattern can be controlled.

IV. Computations and Antenna Characterizations

A. Motivation

First, consider the case of an unperforated substrate. Fig. 2 is a plot of the FDTD computed match $(|S11|)$ of a patch antenna to a 50-Ω transmission line for the cases of 1- and 2-mm-thick substrates. From this data, one can observe the effects of the substrate thickness on the patch resonance. For the thicker substrate, there are decreases in both the frequency and Q of the resonance. The resonance of the patch on the 1-mm-thick substrate is centered at 9.6 GHz with a 1.1% 10-dB bandwidth and the resonance of the patch on the 2-mm-thick substrate is at 8.7 GHz with a 4.3% 10-dB bandwidth.

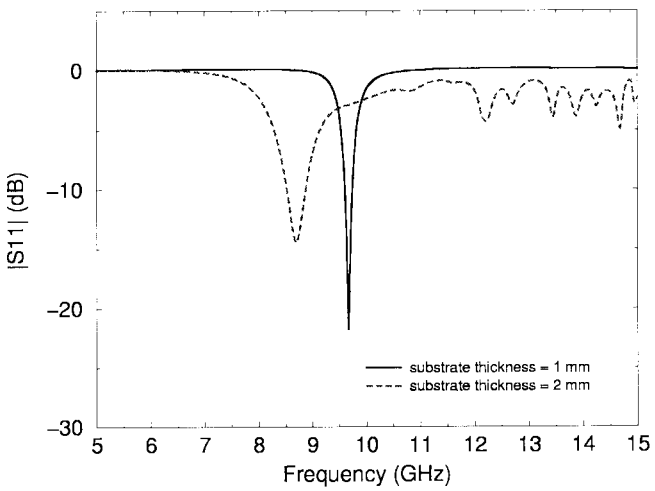

Fig. 2. FDTD computed match to a 50-Ω transmission line for similar patch antennas on 1- and 2-mm-thick substrates. For the patch antenna on the 1-mm substrate the resonance is centered at 9.6 GHz with a 1.1% 10-dB bandwidth and for the patch antenna on the 2-mm substrate the resonance is centered at 8.7 GHz with a 4.3% bandwidth.

Both the downshift in the resonant frequency and increased bandwidth are desirable features. These effects are a result of the reduced coupling of the fields under the patch, i.e., increased fringing. The ripple in the 2-mm-thick substrate $|S11|$ data shown in Fig. 2 above the resonant frequency of the patch is associated with substrate propagation.

Fig. 3(a) and (b) shows plots of the E- and H-plane far-field patterns for these two cases. For both cases, the patterns were computed at the resonant frequency of the patch and the electrical size of the ground plane was kept approximately $1.2\lambda_o \times 1.2\lambda_o$. From the pattern plots shown in Fig. 3, an undesirable directivity drop in the far-field radiation pattern has developed along the z-axis for the case of the 2-mm substrate. Additionally, the thicker substrate resulted in significantly more back radiation in the H plane. Although the exact mechanism for this degradation in the far-field radiation cannot be specified with the FDTD technique, it has been associated with increases in substrate mode edge scattering, because thicker substrates are known to increase the fraction of energy coupled into these substrate modes. This argument is strengthened with the introduction of the results for the patch antenna with perforations in the substrate to follow.

The goal of this research was to achieve a patch design with the same bandwidth and physical size as the 2-mm substrate patch without the directivity drop in the far-field pattern along the z-axis. In the following sections many different far-field pattern cuts and overlays are presented in order to characterize the effects of ground plane size and substrate perforation have on far-field radiation of a patch antenna.

B. Patch and Perforation Separation Effects on Resonance Frequency

Next, the perforation is introduced in the substrate. Fig. 4 is a plot of the computed match of the patch antenna on the 2-mm-thick substrate to a 50-Ω transmission line as a function of the dimension d, as defined in Fig. 1. For reference, the data

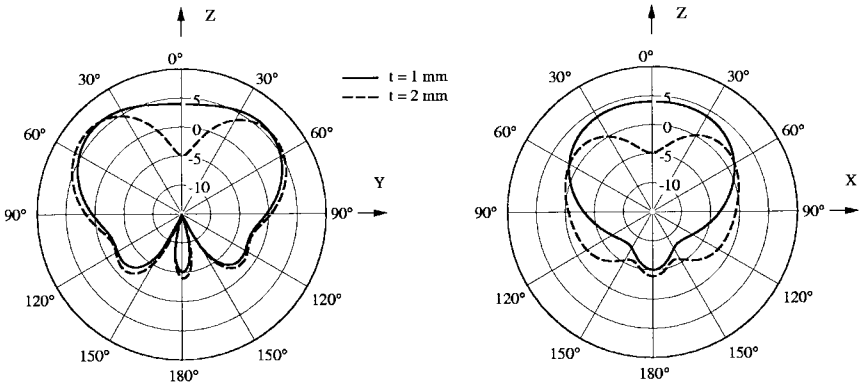

(a) (b)

Fig. 3. FDTD computed far-field patterns for similar patch antennas on a $1.2\lambda_o \times 1.2\lambda_o$ ground plane with a 1- and 2-mm-thick substrates. (a) E-plane. (b) H-plane. For the 2-mm case, notice the approximately 9-dB drop in the broadside directivity.

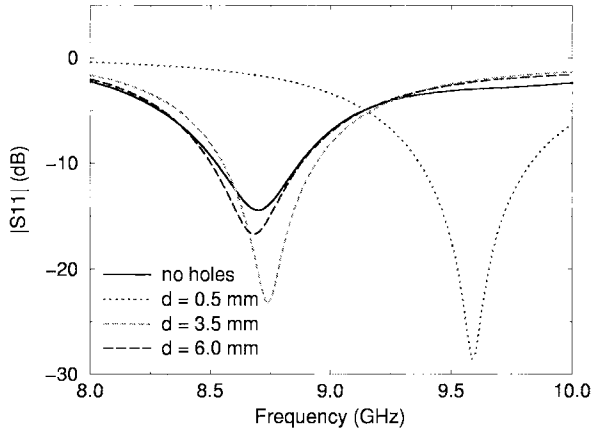

Fig. 4. FDTD computed match, to a 50-Ω transmission line, for a patch antenna on a 2-mm thick substrates for various values of d, as defined in Fig. 1.

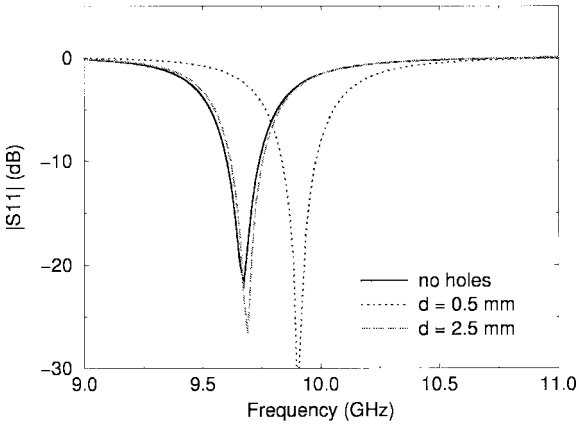

Fig. 5. FDTD computed match to a 50-Ω transmission line for a patch antenna on a 1-mm-thick substrates for various values of d, as defined in Fig. 1.

for the case of no holes in the substrate is also shown. Note for small d there is a considerable shift in the resonance frequency, which is expected due to the fringing of the fields into the perforation region. This fringing into the perforation region results in a lower effective dielectric constant of the material under the patch and, thus, an upward shift in the resonant frequency. As the distance d is increased, there is less fringing into the perforation region and, thus, the resonant frequency shifts back down in frequency. For $d = 6$ mm, the resonance frequency had shifted back to the original resonance frequency of 8.7 GHz and larger values of d do not affect the resonance frequency. The 10-dB bandwidths for the resonances shown in Fig. 4 are as follows: 4.3% for no holes, 4.5% for $d = 6$ mm, 4.6% for $d = 3.5$ mm, and 4.9% for $d = 0.5$ mm. This trend in bandwidth is expected, as the effective dielectric constant of the material under the patch decreases, so will the Q of the resonance.

Fig. 5 shows results for a similar exercise as discussed above, except for the case of a 1-mm-thick substrate. Again, it is seen there is a shift up in resonance frequency for very small values of d and as the value of d increases the resonance shifts down in frequency. For the thinner substrate, the frequency shift of the resonance due to the introduction of the perforation is less severe because the fields do not extend as far from under the patch as the substrate height is decreased.

From the data shown in Figs. 4 and 5, it was determined the smallest acceptable value of d for the 2- and 1-mm-thick substrates was 3.5 and 2.5 mm, respectively. These minimum values for d were chosen as such because they were the smallest values that yielded a match no worse than the original patch designs at the center of the original resonance.

C. Far-Field Radiation Characteristics

Fig. 6(a) and (b) are plots of the far-field radiation for the patch antenna on a $1.2\lambda_o \times 1.2\lambda_o$ ground plane, 2-mm-thick substrate for the case of $d = 3.5$ mm, $d = 10.5$ mm, $d = 15$ mm, and no holes for comparison. For these geometries, the far-field patterns were computed at 8.7 GHz, which makes the ground plane 41.4 mm $\times$ 41.4 mm.

From these figures note that for $d = 3.5$ mm most of the pattern degradation caused by the thicker substrate has been corrected. Comparing the $d = 3.5$ mm data shown in Fig. 6(a) and (b) with the 1-mm-thick substrate patterns shown in Fig. 3(a) and (b), one can see significant correlation

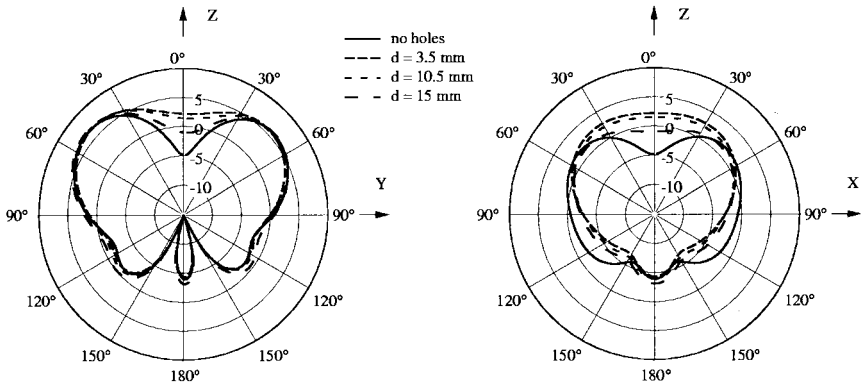

(a) (b)

Fig. 6. FDTD computed far-field patterns for the patch antenna with a 2-mm-thick substrate and a $1.2\lambda_o \times 1.2\lambda_o$ ground plane for various values of d—the distance from the edge of the patch to the point at which the perforation starts. (a) E-plane. (b) H-plane. In these simulations, the value of e was fixed to zero. Note the 7.5-dB improvement in boresight directivity for the case of $d = 3.5$ mm.

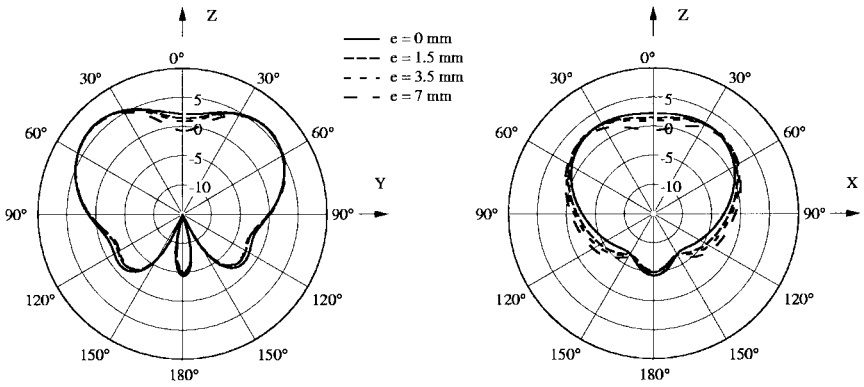

(a) (b)

Fig. 7. FDTD computed far-field patterns for the patch antenna on a $1.2\lambda_o \times 1.2\lambda_o$ ground plane and 2-mm substrate for various values of e, the distance from the edge of the ground plane to the point at which the perforation starts. (a) E-plane. (b) H-plane. In these simulations, the value of d was fixed to 3.5 mm.

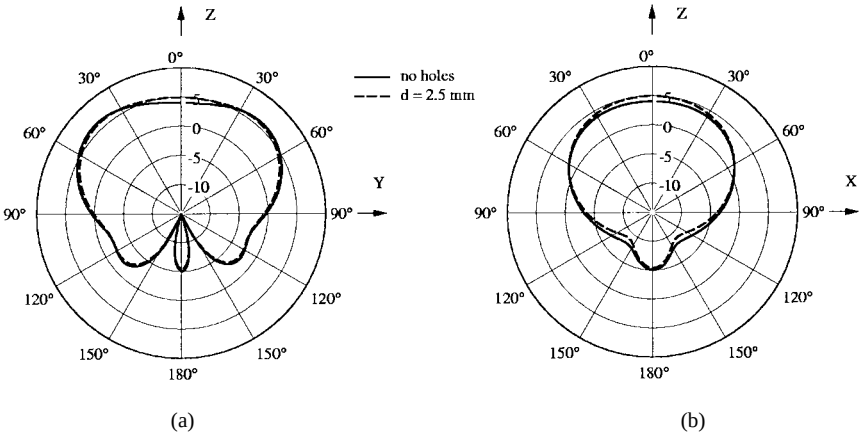

(a) (b)

Fig. 8. FDTD computed far-field patterns for the patch antenna with and without holes in the substrate. In these simulations a 1-mm-thick substrate $d = 2.5$ mm and $1.2\lambda_o \times 1.2\lambda_o$ ground plane were used. (a) E-plane. (b) H-plane. In these simulations, the value of e was fixed to zero.

in their far-field radiation characteristics. Because adding the perforation to the 2-mm-thick substrate was able to retrieve the desired pattern exhibited by the patch on the 1-mm-thick substrate, it suggests the perforation overcomes some of the drawbacks of the thicker substrate. Although, it can also be seen from the data plotted in Fig. 6(a) and (b) that the location of the inner edge of perforation region does have an influence on the far-field pattern and for this case as the edge of the perforation is moved further from the edge of the patch the boresight pattern dip returns.

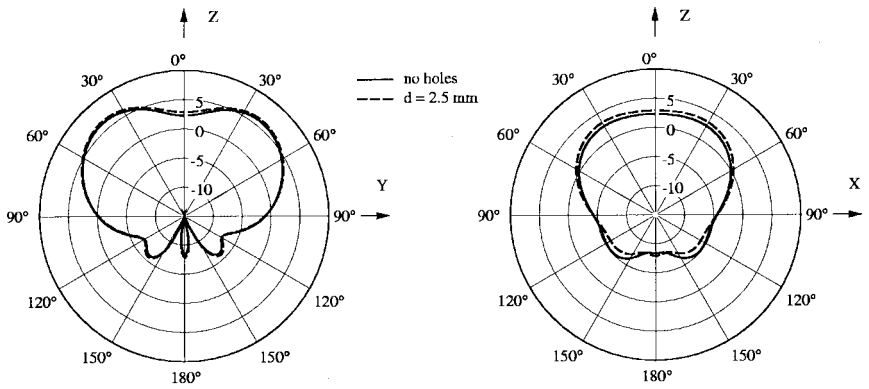

Fig. 9. FDTD computed far-field patterns for the patch antenna with and without holes in the substrate. In these simulations, a 1-mm-thick substrate $d = 2.5$ mm and $1.4\lambda_o \times 1.4\lambda_o$ ground plane were used. (a) E-plane. (b) H-plane. In these simulations, the value of e was fixed to zero.

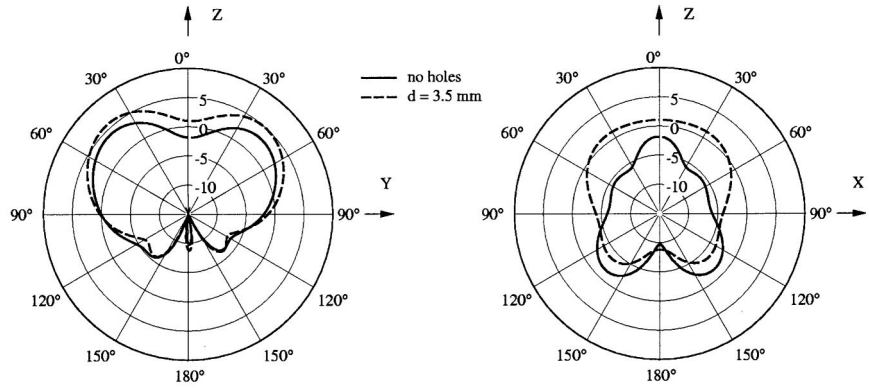

Fig. 10. FDTD computed far-field patterns for the patch antenna with and without holes in the substrate. In these simulations, a 2-mm-thick substrate, $d = 3.5$ mm and $1.4\lambda_o \times 1.4\lambda_o$ ground plane were used. (a) E-plane. (b) H-plane. In these simulations, the value of e was fixed to zero.

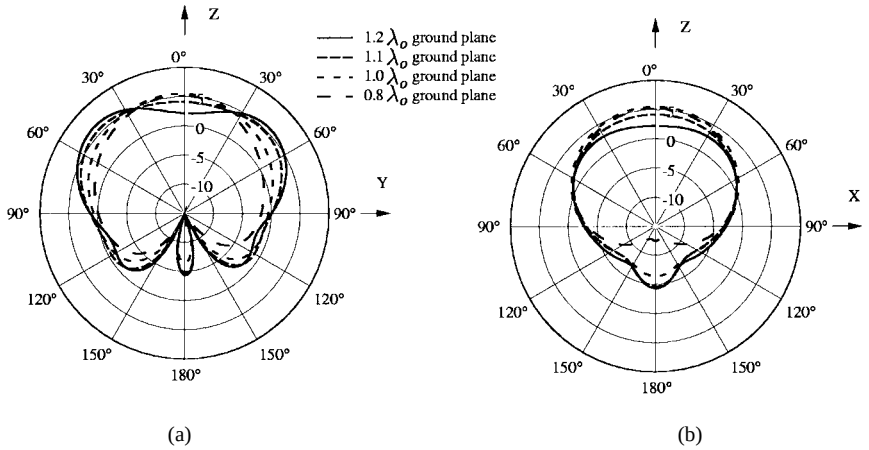

Fig. 11. FDTD computed far-field patterns for the patch antenna on variable sized ground planes and a substrate thickness of 2 mm. Each of the ground planes sizes correspond to the outer area of the perforation region shown in Fig. 7. (a) E-plane. (b) H-plane. In these simulations, the value of d was fixed to 3.5 mm.

Another aspect studied was the effect the location of the outer edge of the perforation relative to the edge of the ground plane had on the far-field radiation properties of the patch antenna. To test this, the value of d was fixed at 3.5 mm and the value of e was varied. The dimension e, denoted in Fig. 1, represents the distance from the edge of the ground plane to the point where the perforation is stopped. In all the results shown previously, the value of e was zero, which means the perforation extended all the way to the outer edge of the ground plane. Fig. 7(a) and (b) are plots of the computed

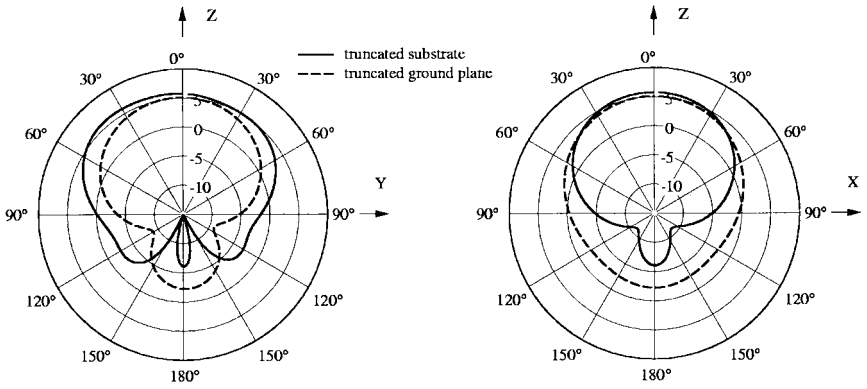

Fig. 12. FDTD computed far-field patterns for the patch antenna on a $0.4\lambda_o \times 0.4\lambda_o$ ground plane with a 2-mm-thick substrate; on a $1.2\lambda_o \times 1.2\lambda_o$ ground plane with the 2-mm-thick substrate truncated to the center $0.4\lambda_o \times 0.4\lambda_o$ region. (a) E-plane. (b) H-plane.

far-field in the E- and H-plane for the patch antenna on the $1.2\lambda_o \times 1.2\lambda_o$ ground plane and 2-mm-thick substrate, respectively, for various values of e with the value of d fixed at 3.5 mm. From this data it can be seen that the perforation does not have to extend all the way to the edge of the ground plane to yield most of its benefit, although moving the outer edge of perforation inwards does cause some degradation in the far-field radiation. These results indicate the length of the perforation region affects the performance improvement achieved, with more being better for this particular case but with saturation in the improvement seen.

The data presented in Figs. 6 and 7 shows that where the perforation region starts and terminates does influence the resulting far-field radiation pattern. This could be because there is some direct radiation of the energy trapped in the substrate modes at the transition in the dielectric constant, thus, the position of the transitions relative to the patch affects the far-field pattern or it is possible the width of the perforation region has an effect on the far-field radiation, possibly because a leaky wave exists in this region. In any event, although all the effects of the substrate propagation cannot be eliminated, the effects on the far-field pattern can be controlled to some extent with the substrate perforation.

Next, consider the computed far-field radiation patterns shown in Figs. 8–10. These plots are direct comparisons of three sets of data: the case of the 1-mm substrate without holes and with holes $d = 2.5$ mm both on a $1.2\lambda_o \times 1.2\lambda_o$ ground plane; the case of the 1-mm substrate without holes and with holes, $d = 2.5$ mm both on a $1.4\lambda_o \times 1.4\lambda_o$ ground plane; the case of the 2-mm substrate without holes and with holes, $d = 3.5$ mm both on a $1.4\lambda_o \times 1.4\lambda_o$ ground plane. In all these simulations the value of e was zero.

From both sets of patterns shown in Figs. 8 and 9 it can be seen that the effect of the holes for the case of the 1 mm thick substrate is not significant. Whereas for the 2 mm thick substrate cases, shown in Fig. 6, ($1.2\lambda_o \times 1.2\lambda_o$ ground plane) and Fig. 10, the substrate perforation has a significant impact on the far-field radiation. For the thick substrate, the perforation helps fill in the pattern dip at zenith. Comparing the results shown in Fig. 8(a) and (b) to the results shown in Fig. 6(a) and (b) and similarly comparing the results shown in Fig. 9(a) and (b) to the results shown in Fig. 10(a) and (b), shows the similarity of the far-field radiation of the 2-mm-thick substrate with holes to the far-field radiation of the 1-mm-thick substrate patch antennas. This indicates the presences of the perforation helps mitigate some of the ill effects of the thicker substrate on the patch antennas radiation performance.

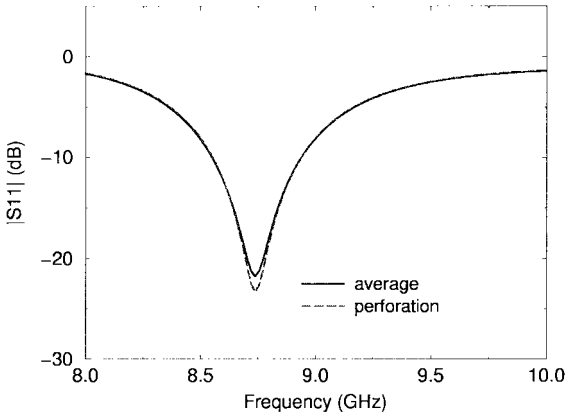

Fig. 13. FDTD computed match to a 50-Ω transmission line for a patch antenna on a 2-mm-thick substrates for the cases of substrate perforation of $d = 3.5$ mm and the perforation replaced by a solid piece of $\epsilon_r = 5.3$ dielectric. Both these designs have computed resonances centered at 8.7 GHz with 4.6% 10-dB bandwidths.

D. Ground Plane and Substrate Size

Fig. 11(a) and (b) are plots of the far-field radiation for the patch antenna on the 2-mm-thick perforated substrate $d = 3.5$ mm for various sized ground planes: $1.2\lambda_o \times 1.2\lambda_o$; $1.1\lambda_o \times 1.1\lambda_o$; $1.0\lambda_o \times 1.0\lambda_o$; and $0.8\lambda_o \times 0.8\lambda_o$. In these simulations, the perforation was extended to the the outer edge of the ground plane. The ground plane sizes of these geometries correspond to the outer edge of the perforation regions for the simulations depicted in Fig. 7(a) and (b). Comparing the results shown in Fig. 11(a) and (b) with those shown in Fig. 7(a) and (b), it is clearly seen truncating the perforation results in different radiation characteristics than truncating the ground plane at the same location.

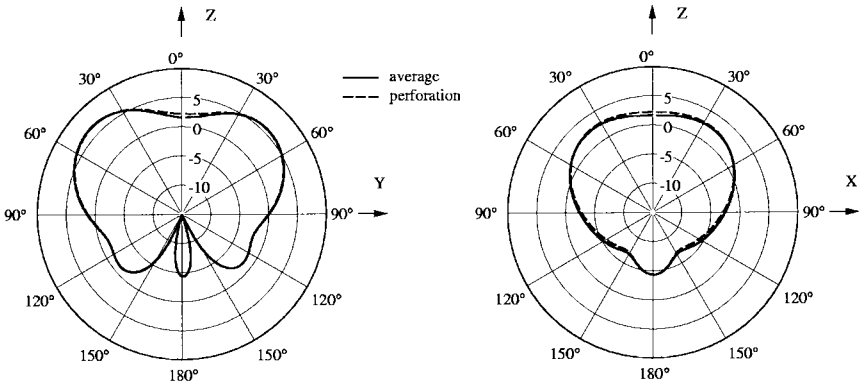

Fig. 14. FDTD computed far-field patterns for the patch antenna on a $1.2\lambda_o \times 1.2\lambda_o$ ground plane and 2-mm-thick substrate for both the case of substrate perforation and the volumetric average dielectric constant. (a) E-plane. (b) H-plane. In these simulations, the value of d was fixed to 3.5 mm and e to zero.

Fig. 12 shows the computed far-field radiation characteristics for the patch antenna on an unperforated 2-mm-thick substrate on a $0.4\lambda_o \times 0.4\lambda_o$ ground plane and on a $1.2\lambda_o \times 1.2\lambda_o$ ground plane with the substrate limited to the center $0.4\lambda_o \times 0.4\lambda_o$ portion of the ground plane. This latter case is obviously the largest change in substrate dielectric constant that can be achieved with the perforation technique, the case for which the hole size becomes larger than the hole separation. For the case of $d = 3.5$ mm shown in Fig. 6(a) and (b), the unperturbed region of the substrate is the center $0.37\lambda_o \times 0.42\lambda_o$ portion. From these results, it is again clear that the ground plane size has a large effect on the far-field radiation characteristics, independent of where the substrate is truncated. Note, the case of the substrate trucated to the center $0.4\lambda_o \times 0.4\lambda_o$ portion of the ground plane, in fact, gives the highest value of boresight directivity for the particular geometry considered in this work.

E. Effective Dielectric Constant

As suggested previously, the perforation introduced into the substrate around the patch antenna has been viewed in terms of lowering the effective dielectric constant of the surrounding substrate. From previous work, it has been found that a good estimate of the effective dielectric constant for the perforated dielectric material when the hole separation is less then $\lambda/2$ in the substrate material is the volumetric average. For the hole size and layout used in this work, the volumetric average of the 10.2 material and the free-space holes is 5.3. Using the FDTD technique, the same patch antenna can be easily simulated with the perforation region of the substrate replaced with solid dielectric material of $\epsilon_r = 5.3$. Figs. 13 and 14 are overlays of impedance and pattern data directly comparing the results obtained with the use of substrate perforation to the case of its replacement with solid $\epsilon_r = 5.3$ material. From the strong correlation exhibited in these data sets, the volumetric average model appears to hold.

V. Antenna Fabrication and Measured Results

To verify some of the conclusions drawn from the FDTD simulations, three separate patch antennas were fabricated on

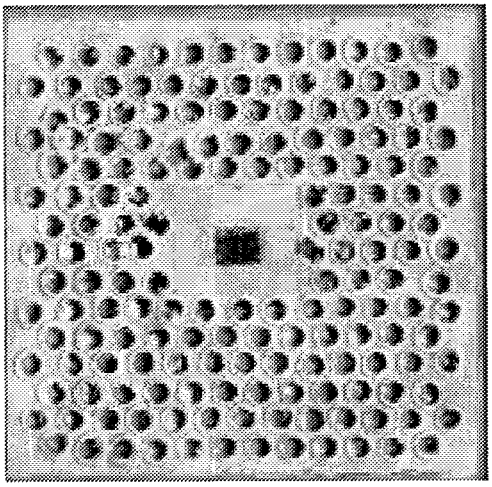

Fig. 15. Photo of one of the fabricated patch antennas with external substrate perforation. The substrate material has a dielectric constant of $\epsilon_r = 10.2$ and the hole diameter is 2.1 mm. Within each column, the center to center distance is 3 mm and the column-to-column center separation is 2.5 mm. Adjacent columns of holes are shifted half a period respect to each other.

Rogers RT/Duroid 6010 ($\epsilon_r = 10.2$) substrate material. One antenna was fabricated on a 0.63-mm (25 mil)-thick substrate, the other two on a 1.9-mm (75 mil) substrate material. All three antennas were fed through the ground plane with a coax probe.

Of the three antennas fabricated, substrate perforation was added to one of the 1.9-mm substrate. The substrate perforation was realized by drilling a precision set of holes into the subtrates. The dimensions of the hole pattern drilled were that simulated, the only difference being the shape of the holes. Whereas square holes 2 mm on a side were simulated, the perforation realized was a set of circular hole with a 2.2-mm diameter. Although the hole shapes were different, the volume fraction of material removed were approximately the same for the simulated and fabricated substrates. Note, in the volumetric model proposed for the perforated substrates, the shape of the holes is not important only the effective volumetric average dielectric constant of the substrate. This was found to be true in FDTD simulations as long as the hole spacing remained

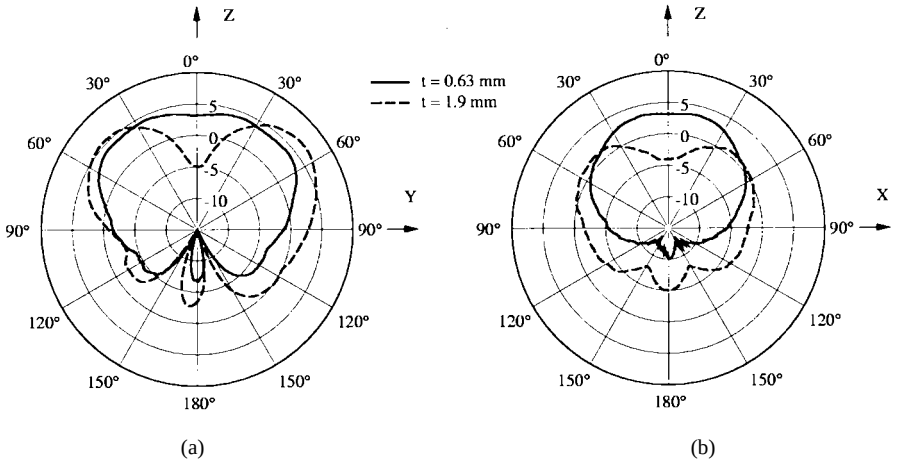

Fig. 16. Measured far-field patterns for similar patch antennas on a $1.2\lambda_o \times 1.2\lambda_o$ ground plane with 0.63- and 1.9-mm-thick substrates. (a) E-plane. (b) H-plane.

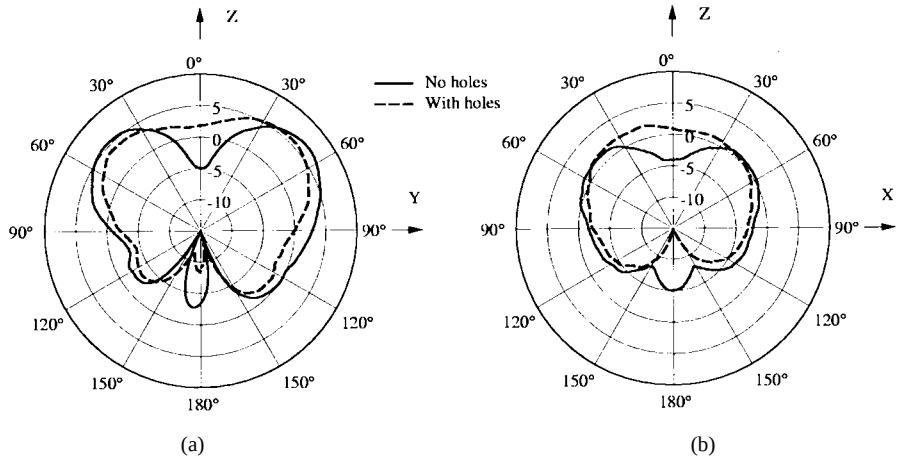

Fig. 17. Measured far-field patterns for the patch antenna on a $1.2\lambda_o \times 1.2\lambda_o$ ground plane with and without holes in the 1.9-mm-thick substrate. (a) E-plane. (b) H-plane.

less than half a dielectric wavelength. The placement of each hole drilled was measured by a digital output on the drill press used. The holes were drilled completely through the substrate and ground plane and then conducting tape was added to the backside of the ground plane to effectively fill the holes in the ground plane back in, leaving only the holes in the substrate. Fig. 15 shows a photograph of the fabricated patch antennas with substrate perforation. After being built, the resonant frequency of each antenna was measured and the ground plane then cut to ensure it was 1.2 λ_o by $1.2\lambda_o$ at the measured resonant frequency. The measured resonant frequencies and input match correlated well with the simulations.

Fig. 16(a) and (b) are plots of the measured E- and H-plane patterns of the patch antennas on the 0.63- and 1.9-mm-thick substrates without substrate perforation. The pattern dip predicted in the FDTD simulations [see Fig. 3(a) and (b)] can be observed in these measured results as well.

Fig. 17(a) and (b) shows plots of the measured E- and H-plane patterns for the patch antennas fabricated on the 1.9-mm-thick substrate with and without substrate perforation. As seen in the FDTD simulation results [see Fig. 6(a) and (b)], adding the perforation to the thick high dielectric constant substrate helped fill in the undesireable pattern dip at boresight. Much of the differences between the measured patterns shown in Fig. 17(a) and (b) and the computed patterns shown in Fig. 6(a) and (b) can be attributed to fabrication errors.

VI. Conclusions

In this paper, the idea of external substrate perforation was introduced and applied to a patch antenna to help mitigate the drawbacks of thick high dielectric constant substrates without sacrificing the patch element miniaturization or bandwidth. From the results presented, the introduction of the external perforation improved the far-field radiation pattern of a patch antenna on a relatively thick substrate without any reduction in bandwidth or increase in patch size. This result was drawn from comparison to a similar patch antenna on a thinner substrate, and observed in both FDTD simulations and measurements

The improvement in the far-field radiation pattern has been attributed to the reduction of the edge scattered component from the energy trapped in the substrate. This was accomplished by lowering the effective dielectric constant of the

substrate surrounding the patch. Thus, this change in substrate dielectric constant decreased the amount of energy incident upon the edge of the ground plane via substrate propagation. The effective dielectric constant of the substrate surrounding the patch was lowered by introducing an array of small closely spaced holes.

Various aspects of the exact layout of the perforation relative to the patch and ground plane were explored. It was found that the perforation must not be located too close to the patch due to fringing fields, or the resonant frequency would shift up. It was also seen that the position where the perforation is started or terminated does have some affect on the far-field radiation pattern.

Future research will study optimum dielectric constant profile designs for various applications. One application of great interest is patch antenna arrays, where substrate dielectric constant profile design can be used to reduce element to element interactions.

ACKNOWLEDGMENT

The authors would like to thank Z. Li for fabricating the antennas and performing the measurements.

REFERENCES

[1] R. Coccioli, W. R. Deal, and T. Itoh, "Radiation characteristics of a patch antenna on a thin PBG substrate," in *1998 IEEE AP-S Dig.*, Atlanta, GA, June 1998, pp. 656–659.
[2] P. K. Kelly, M. Picket-May, I. Rumsey, and A. Bhobe, "Microstrip patch antenna performance on a photonic bandgap substrate," in *1998 USNC/URSI Nat. Radio Sci. Meet. Dig.*, Atlanta, GA, June 1998, p. 5.
[3] K. Agi, K. J. Malloy, E. Schamiloglu, and M. Mojahedi, "Compact microstrip patch on photonic crystal substrates," in *1998 USNC/URSI Nat. Radio Sci. Meet. Dig.*, Atlanta, GA, June 1998, p. 119.
[4] D. R. Jackson and J. T. Williams, and A. K. Bhattacharyya, "Microstrip patch designs that do not excite surface waves," *IEEE Trans. Antennas Propagat.*, vol. 41, pp. 1026–1037, Aug. 1993.
[5] M. J. Vaughan, K. Y. Hur, and R. C. Compton, "Improvements of microstrip patch antenna radiation patterns," *IEEE Trans. Antennas Propagat.*, vol. 42, pp. 882–885, June 1994.
[6] M. Stotz, G. Gottwald, and H. Haspeklo, "Planar millimeter wave antennas using SiN_x-membranes on GaAs," *IEEE Trans. Microwave Theory Tech.*, vol. 44, pp. 1593–1596, Sept. 1996.
[7] J. B. Muldavin, T. J. Ellis, and G. M. Rebeiz, "Taper slot antennas on thick dielectric substrates using micromachining techniques," in *1997 IEEE AP-S Dig.*, Montreal, Canada, July 1997, pp. 1110–1113.
[8] G. P. Gauthier, A. Courtay, and G. H. Rebeiz, "Microstrip antennas on synthesized low dielectric-constant substrate," *IEEE Trans. Antennas Propagat.*, vol. 45, pp. 1310–1314, Aug. 1997.
[9] J. S. Colburn and Y. Rahmat-Samii, "Printed antenna pattern improvement through substrate perforation of high dielectric constant material: An FDTD evaluation," *Microwave Opt. Technol. Lett.*, vol. 18, p. 1, May 1998.
[10] J. B. Birks and J. H. Schulman, *Progress in Dielectrics*. New York: Wiley, 1960, p. 2.
[11] M. A. Jensen and Y. Rahmat-Samii, "Performance analysis of antennas for hand-held transceivers using FDTD," *IEEE Trans. Antennas Propagat.*, vol. 42, no. 8, pp. 1106–1113, Aug. 1994.
[12] R. F. Harrington, *Time-Harmonic Electromagnetic Fields*. New York: McGraw-Hill, 1961.
[13] J. Huang, "The finite ground plane effect on the microstrip antenna radiation patterns," *IEEE Trans. Antennas Propagat.*, vol. AP-31, pp. 649–653, July 1983.
[14] S. Maci, L. Borselli, and L. Rossi, "Diffraction at the edge of a truncated grounded dielectric slab," *IEEE Trans. Antennas Propagat.*, June 1996, vol. 44, pp. 863–873.
[15] D. H. Schaubert and K. S. Yngvesson, "Experimental study of a microstrip array on high permittivity substrate," *IEEE Trans. Antennas Propagat.*, vol. AP-34, pp. 92–97, Jan. 1986.
[16] M. F. Otero and R.G. Rojas, "Analysis and treatment of edge effects on the radiation pattern of a microstrip patch antenna," in *1995 IEEE AP-S Dig.*, Newport Beach, CA, June 1995, p. 1050.

Joseph S. Colburn (S'91–M'98) received the B.S. degree (*summa cum laude*) from the University of Washington, Seattle, in 1992, and the M.S. and Ph.D. degrees from the University of California, Los Angeles (UCLA), in 1994 and 1998, respectively, all in electrical engineering.

From 1993 to 1995 and 1997 to 1998, he was employed by the Department of Electrical Engineering, UCLA, both as a Research Assistant in the UCLA Antenna Laboratory and as a Teaching Assistant. From 1995 to 1997 he was with TRW Space and Electronics Group, Redondo Beach, CA, where he worked as an Antenna Engineer. He is currently with HRL Laboratories, Malibu, CA, working on antenna analysis and design. His research interests include radiation and propagation issues in wireless communications, and related topics in numerical electromagnetics.

Yahya Rahmat-Samii (S'73–M'75–SM'79–F'85), for a photograph and biography, see p. 583 of the March 1999 issue of this TRANSACTIONS.